

Article

Effect of Poly(Vinyl Alcohol) Concentration and Chain Length on Polymer Nanogel Formation in Aqueous Dispersion Polymerization

Yukiya Kitayama ^{1,2,*} , Shunsuke Takigawa ¹ and Atsushi Harada ^{1,2,*} 

¹ Department of Applied Chemistry, Graduate School of Engineering, Osaka Prefecture University, 1-1 Gakuen-cho, Naka-ku, Sakai, Osaka 599-8531, Japan

² Department of Applied Chemistry, Graduate School of Engineering, Osaka Metropolitan University, 1-1 Gakuen-cho, Naka-ku, Sakai, Osaka 599-8531, Japan

* Correspondence: kitayama@omu.ac.jp (Y.K.); atsushi_harada@omu.ac.jp (A.H.)

Abstract: Nanotechnology has attracted increasing interest in various research fields for fabricating functional nanomaterials. In this study, we investigated the effect of poly(vinyl alcohol) (PVA) addition on the formation and thermoresponsive properties of poly(*N*-isopropyl acrylamide)-based nanogels in aqueous dispersion polymerizations. During dispersion polymerization, PVA appears to play three roles: (i) it bridges the generated polymer chains during polymerization, (ii) it stabilizes the formed polymer nanogels, and (iii) it regulates the thermoresponsive properties of the polymer nanogels. By regulating the bridging effect of PVA via changing the PVA concentration and chain length, the size of the obtained polymer gel particles was maintained in the nanometer range. Furthermore, we found that the clouding-point temperature increased when using low-molecular weight PVA. We believe that the knowledge gained in this study regarding the effect of PVA concentration and chain length on nanogel formation will aid in the future fabrication of functional polymer nanogels.

Keywords: nanogel; colloid; polymer; thermoresponsiveness; poly(vinyl alcohol)



Citation: Kitayama, Y.; Takigawa, S.; Harada, A. Effect of Poly(Vinyl Alcohol) Concentration and Chain Length on Polymer Nanogel Formation in Aqueous Dispersion Polymerization. *Molecules* **2023**, *28*, 3493. <https://doi.org/10.3390/molecules28083493>

Academic Editor: Ali Nazemi

Received: 13 March 2023

Revised: 4 April 2023

Accepted: 13 April 2023

Published: 15 April 2023



Copyright: © 2023 by the authors. Licensee MDPI, Basel, Switzerland. This article is an open access article distributed under the terms and conditions of the Creative Commons Attribution (CC BY) license (<https://creativecommons.org/licenses/by/4.0/>).

1. Introduction

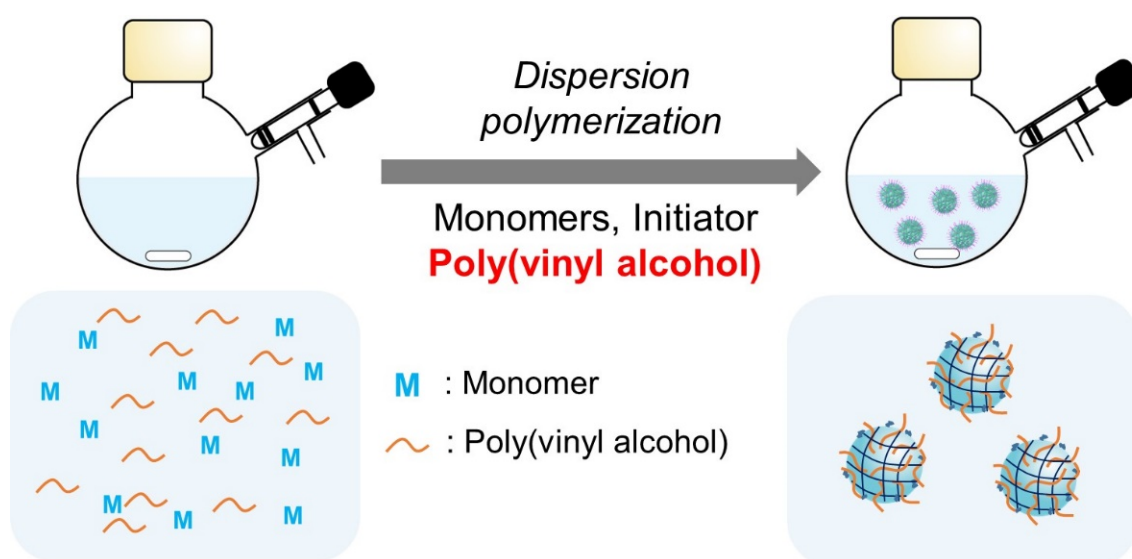
Nanomaterials are employed in a wide range of applications, such as biomedical applications [1–7], catalysts [8], water treatment [9], and dye-adsorbents [10]. Polymer-based nanomaterials are highly attractive because they can be functionalized using a wide range of functional building blocks (monomers) and post-polymerization modifications. Aqueous heterogeneous polymerization systems, such as miniemulsion [11–14], emulsion [15–20], dispersion [21–24], and precipitation polymerizations [25–28], are attractive approaches for preparing polymer-based particulate materials from monomer species directly in aqueous media. Among these, dispersion polymerizations with biocompatible stabilizers and precipitation polymerization are attractive for preparing polymeric nanomaterials for bio-related applications. Utilizing these polymerization systems, poly(*N*-isopropyl acrylamide) (PNIPAm)-based microgels/nanogels can be prepared in aqueous media. The PNIPAm-based microgels/nanogels exhibit thermoresponsive properties, owing to the lower critical solution temperature (LCST)-type phase transition property of PNIPAm.

Several researchers have investigated the effect of stabilizers on the particle size and thermoresponsive properties of polymer microgels in the dispersion polymerizations. Among a wide range of stabilizers, poly(vinyl alcohol) (PVA) is a representative biocompatible water-soluble stabilizer in the dispersion polymerizations. In the presence of PVA, the radical chain transfer reaction occurs, and the mid-chain radicals generated on PVA initiate the propagation reaction with monomer species, resulting in covalent grafting of PVA on the polymer gel particles [29]. The grafted PVA chain stabilized polymer particles

via steric repulsion. To date, the effect of PVA on the synthesis of poly(NIPAm)-based microgels in dispersion polymerizations has been investigated [30,31]. Yates et al. reported the synthesis of PVA-stabilized PNIPAm-based microgels [30]. Guan and Zhang reported that the addition of PVA significantly affected the thermoresponsive properties of phenylboronic acid-functionalized PNIPAm-based microgels [31]. Furthermore, they investigated the effect of PVA molecular weights on the thermoresponsiveness of the PNIPAm-based microgels.

Nanometer-sized polymer gels (nanogels) with a particle size <100 nm are widely used in drug delivery systems for cancer treatments because of their passive targeting properties derived from enhanced permeability and retention effects [32]. However, PNIPAm-based gels generally attain (sub)micrometer-sized particles in precipitation polymerizations. Nanogels have been successfully synthesized via dispersion polymerization using sodium dodecyl sulfate (SDS) as a surfactant [33]. However, SDS is harmful for biological applications. Recently, we have successfully demonstrated the synthesis of PNIPAm-based nanogels via precipitation polymerization (without surfactants) under suitable conditions [34–37]. Furthermore, the polymer nanogels can recognize intrinsic dysopsonic proteins (serum albumin) and be employed as novel nanocarriers in drug delivery systems [34,38,39]. These polymer nanogels gain stealth capability in situ in the blood vessel by cloaking themselves with intrinsic serum albumin, resulting in their prolonged circulation in the blood [34]. Furthermore, gold nanoparticle-incorporated polymer nanogels prepared via precipitation polymerization have been successfully used as radiation sensitizers [40]. Therefore, the polymer nanogels prepared by precipitation polymerization have been successfully used as drug delivery carriers.

To the best of our knowledge, no studies examining the effect of PVA addition on polymer nanogel formation have been reported. Herein, we investigated the effect of PVA concentration and chain length on the particle formation and thermoresponsive properties of PNIPAm-based nanogels prepared via aqueous dispersion polymerization (Scheme 1). In a series of experiments, we discovered that PVA plays three roles: (i) it bridges the generated polymer chains during polymerization, (ii) it stabilizes the formed polymer nanogels, and (iii) it regulates the thermoresponsive properties of the polymer nanogels when PVA possessing a low molecular weight (degree of polymerization: 500) is used. We believe that the knowledge gained in this study will aid in the future fabrication of functional polymer nanogels.



Scheme 1. Schematic of preparation of polymer nanogels via aqueous dispersion/precipitation polymerization in the presence of poly(vinyl alcohol).

2. Results and Discussion

2.1. Effect of PVA Addition on Nanogel Formation

Precipitation polymerization was performed without PVA in 10 mM phosphate buffer (pH 7.4) using *N*-isopropyl acrylamide (NIPAm), *t*-butyl acrylamide (TBAm), 2-methacryloyloxyethyl phosphorylcholine (MPC), and *N,N'*-methylenebisacrylamide (MBAA) as monomers. 2,2'-Azobis(2-methylpropionamide) dihydrochloride (V-50) was selected as the water-soluble initiator. All monomer species and the initiator were dissolved in the solvent prior to polymerization. NIPAm-based polymers are thermoresponsive and exhibit LCST-type phase transitions, owing to the polymer dehydration at high temperatures; thus, the polymers precipitated and assembled as particles to decrease the interfacial free energy during polymerization. The polymers were crosslinked by copolymerizing with MBAA as a crosslinking agent. The conversion of this precipitation polymerization, evaluated using ¹H-nuclear magnetic resonance (NMR), was approximately 100%, with the protons of the vinyl groups of the monomers almost disappearing (Figure S1). Using dynamic light scattering (DLS), the average particle size of the obtained polymer nanogels (PG₀) was determined to be approximately 20 nm (Figure 1), which corresponds with that obtained in our previous study [34].

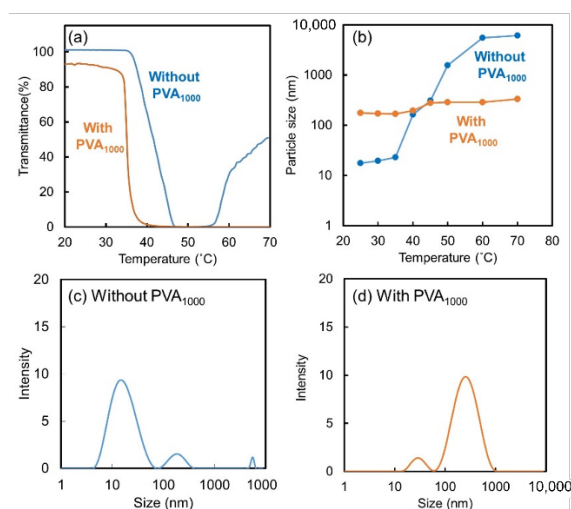


Figure 1. Transmittance (a) and average particle size (b) of PG₀ and PG₁₀₀₀ dispersions at various temperatures. Particle size distributions of obtained PG₀ particles (prepared without PVA₁₀₀₀, (c)) and PG₁₀₀₀ particles (prepared with PVA₁₀₀₀, (d)) at 30 °C. PG₀ and PG₁₀₀₀ particles were prepared via precipitation and dispersion polymerizations with PVA₁₀₀₀ (3 mg/mL) at 70 °C for 3 h.

The thermoresponsiveness of PG₀ was investigated using transmittance measurements. When the temperature reached above the clouding-point temperature of NIPAm-based polymers, their dehydration occurred, resulting in the precipitation of the polymer chains from the aqueous phase. The transmittance of the PG₀ dispersions steeply decreased above 40 °C, whereas their clouding-point temperature (the temperature at which polymers show 50% transmittance (T)) was estimated to be approximately 43 °C (Figure 1). However, the particle size measured using DLS considerably increased to >1000 nm above the clouding-point temperature, indicating that the polymer nanogels coagulated (Figure 1). The nearly neutral zeta potential of the polymer nanogels (approximately 2.3 mV at 25 °C) indicated that PG₀ was stabilized via steric repulsion exhibited by hydrated polymer chains grafted onto the polymer nanogels below the clouding-point temperature, rather than electrostatic repulsion between the cationic chain ends of V-50. However, the polymer chains grafted onto the nanogels do not exhibit steric repulsion above the clouding-point temperature due to dehydration, causing particle coagulation.

To investigate the effect of PVA on the particle formation, PVA₁₀₀₀ (polymerization degree: 1000; average saponification degree: 88%, 3 mg/mL) was added to the polymer-

ization system. PVA is widely used in biomedical applications as a nanocarrier material or bioadhesive because of its low toxicity [41,42]. Therefore, the PNIPAm-based nanogels were prepared in the presence of PVA₁₀₀₀ (PG₁₀₀₀). The conversion reached approximately 100% even in the presence of PVA, as evaluated using ¹H-NMR spectroscopy (Figure S2). This is because the radical concentration in the polymerization system does not significantly change when the radical chain transfer to PVA occurs. The clouding-point temperature of the obtained PG₁₀₀₀ (approximately 40 °C) estimated from the transmittance measurements was similar to that of the PG₀ (approximately 43 °C) (Figure 1), indicating that the additional amount of PVA₁₀₀₀ had no significant effect on the phase transition temperature of the gel particles. The transmittance of the gel particle dispersion was reversibly changed by heating and cooling (Figure S3). However, the particle sizes of PG₀ and PG₁₀₀₀ significantly differ. Below the clouding-point temperature, PG₁₀₀₀ had a larger average particle size (approximately 125 nm) than PG₀ (approximately 20 nm). Above the clouding-point temperature, the average particle size of PG₁₀₀₀ remained constant at approximately 350 nm (Figure 1). The particle size distribution of PG₁₀₀₀ below the clouding-point temperature indicates the bimodal distribution of nanometer-sized and submicrometer-sized particles. However, the particle size distribution was unimodal above the clouding-point temperature (at 60 °C), and the nanometer-sized particles disappeared from the distribution (Figure 2). These results indicate that the nanometer-sized gel particles coagulated with the submicrometer-sized gel particles above the clouding-point temperature. To investigate whether particle coagulation occurred above clouding-point temperatures, particle size measurements were performed after adding a cationic surfactant [cetyltrimethylammonium bromide (CTAB)] because cationic surfactants suppress the coagulation of destabilized particles above the clouding-point temperatures. Notably, above the clouding-point temperature, the particle size of PG₁₀₀₀ did not significantly increase in the presence of a cationic surfactant (Figure S4). These results indicate that the increase in the particle size of PG₁₀₀₀ above the clouding-point temperatures was caused by the coagulation of the destabilized polymer nanogels.

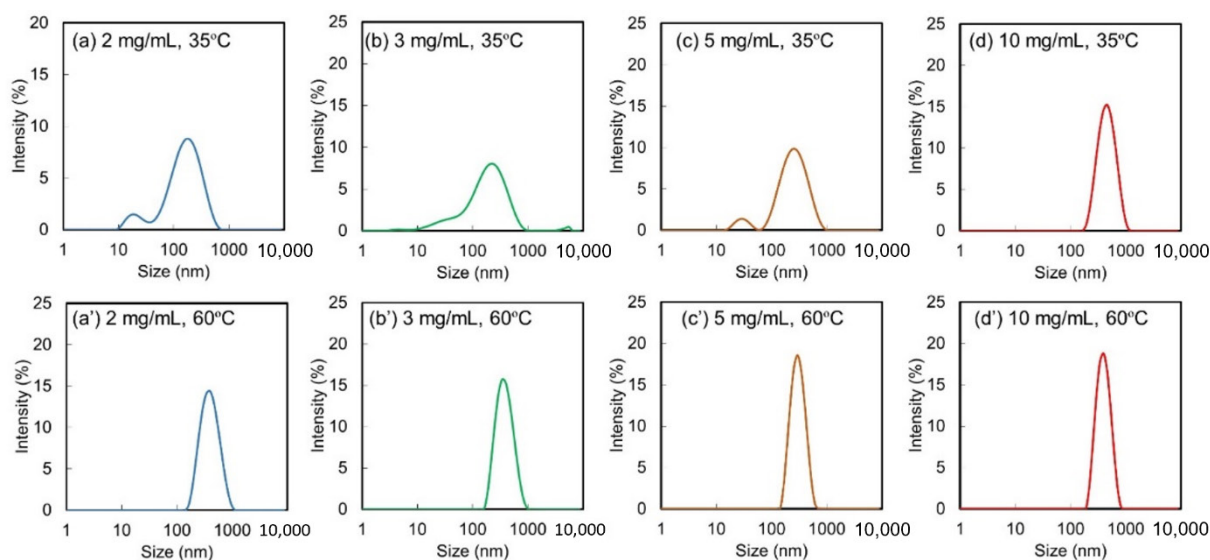
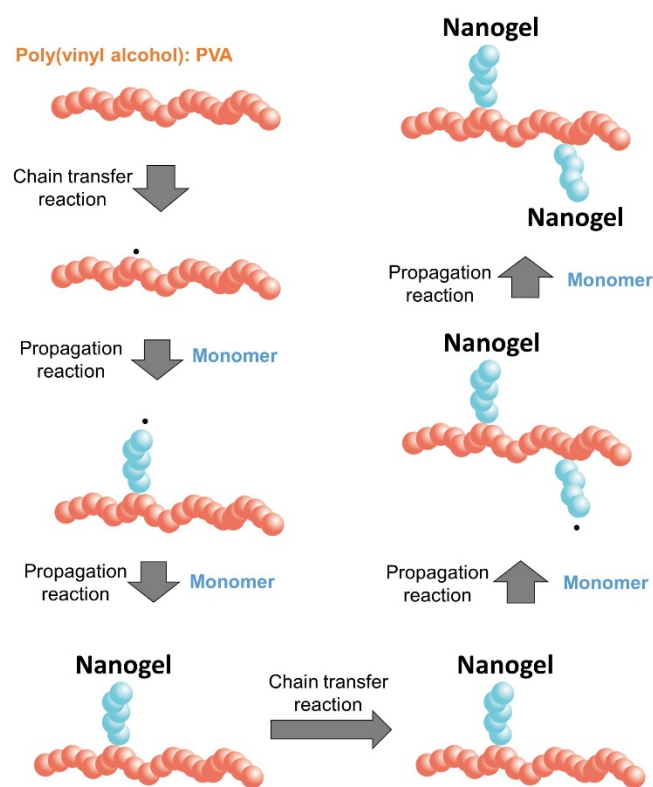


Figure 2. Particle size distributions of PG₁₀₀₀ particles at 35 °C (a–d) and 60 °C (a'–d'). PVA₁₀₀₀ concentrations: 2 (a,a'), 3 (b,b'), 5 (c,c'), and 10 (d,d') mg/mL. PG₁₀₀₀ particles were prepared via dispersion polymerization with different PVA₁₀₀₀ concentrations (2, 3, 5, and 10 mg/mL) at 70 °C for 3 h.

Based on these results, PVA appears to play two roles in the particle formation/stabilization: as a stabilizer (primary role) and as a bridging ligand (secondary role). During polymerization, mid-chain radicals are generated on PVA via a chain transfer reaction, which initiates

the monomer addition reaction. The radical species then undergo a termination reaction with another radical species, yielding dead polymers. During dispersion polymerization, the propagating/dead polymer chains precipitate from the aqueous phase. This series of reactions (chain transfer, propagation, and termination) graft PVA chains on the polymer nanogels, leading to particle stabilization via steric hindrance (primary role of PVA). However, the series of reactions can occur multiple times on the same PVA, inducing bridging between two or more polymer nanogels with a single PVA chain (Scheme 2). The bridging phenomenon (secondary role of PVA) may lead to the formation of submicrometer-sized polymer nanogels.



Scheme 2. Schematic of the bridging effect of PVA between different polymer chains in nanogels.

2.2. Effect of PVA₁₀₀₀ Concentration

Based on the above findings, we can speculate that the submicrometer-sized gel particles were formed via the PVA₁₀₀₀-induced bridging of multiple nanogels, whereas the nanometer-sized gel particles might have formed without the bridging effect. To verify this hypothesis, we investigated the effect of the PVA₁₀₀₀ concentration on particle formation and stabilization. When the PVA₁₀₀₀ concentration was increased from 2 to 10 mg/mL (at 35 °C, below the clouding-point temperature), the average size of the gel particles gradually increased (Figure 3), and the peak corresponding to the nanometer-sized gel particles disappeared when 10 mg/mL of PVA₁₀₀₀ was used (Figure 2). These results indicate that the submicrometer-sized gel particles were formed because of the bridging effect of PVA₁₀₀₀. Notably, the clouding-point temperatures determined using the transmittance measurements were similar for all PVA₁₀₀₀ concentrations, indicating that the PVA₁₀₀₀ concentration did not affect the phase transition temperature of PG₁₀₀₀ during polymerization (Figure S5). Furthermore, the particle size distributions obtained all PVA₁₀₀₀ concentrations were unimodal above the clouding-point temperature (at 60 °C), indicating that the submicrometer-sized polymer gel particles were colloidally stable even above the clouding-point temperature (Figure 2). These results clearly indicate that the addition of PVA₁₀₀₀ led to both the stabilization and bridging of polymer gel particles and/or polymer chains during polymerization (Scheme 3). Thus, the polymer gel particles

may have crosslinked by MBAA and PVA. Furthermore, the grafting density of the polymer gel particles may increase with increasing PVA concentration because PVA can act as a bridging agent (crosslinker) between different nanogel particles and/or polymer chains. However, a detailed investigation is necessary to evaluate the crosslinking density of the polymer gel particles using light or X-ray scattering.

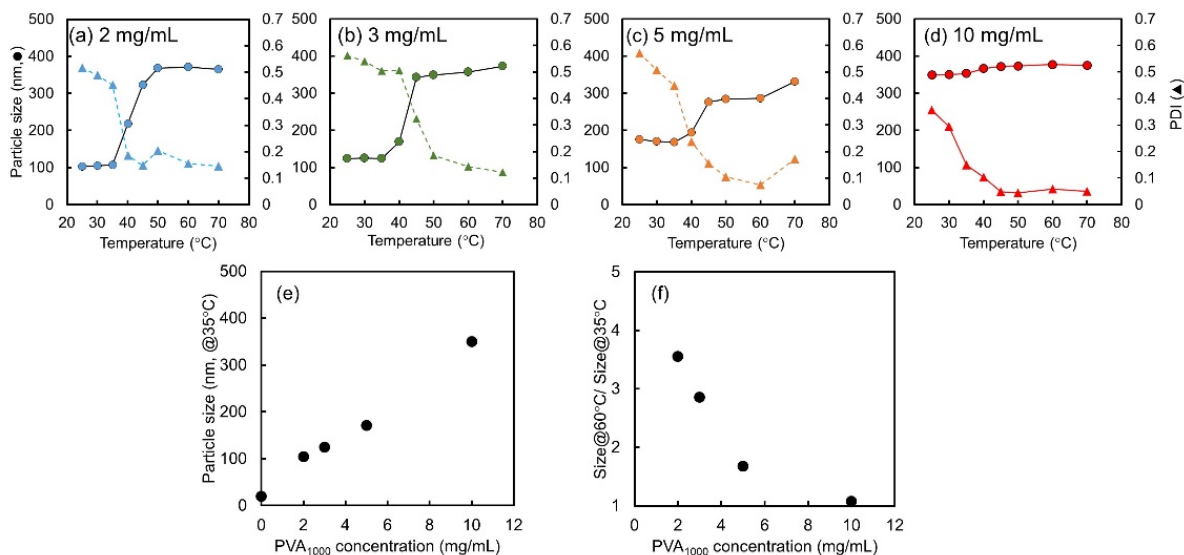
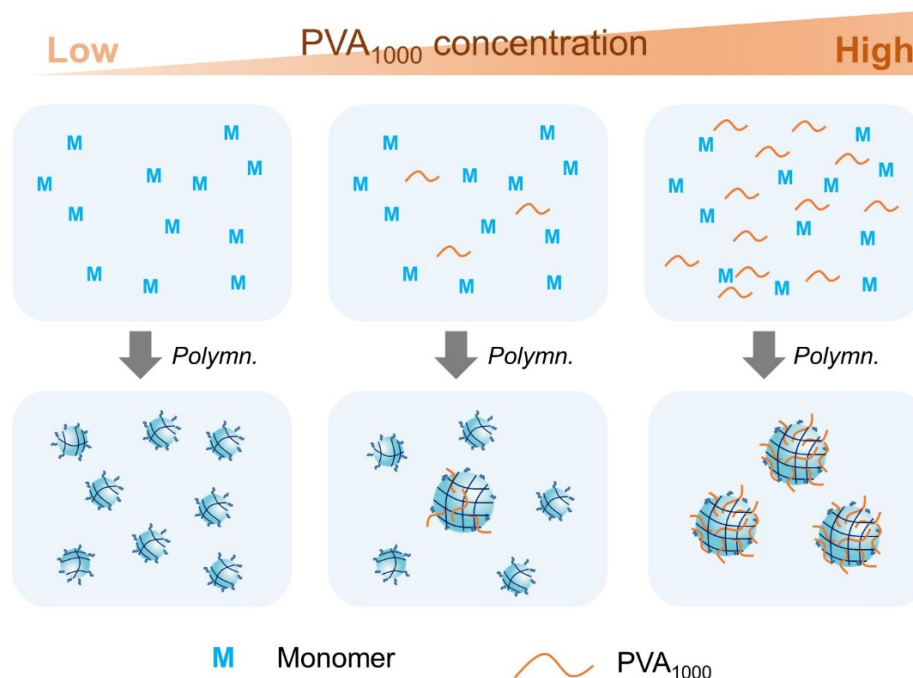


Figure 3. Average particle sizes (circles) and polydispersity index (PDI, triangles) (a–d) of PG₁₀₀₀ particles at various temperatures, where PG₁₀₀₀ particles were prepared with 2 (a), 3 (b), 5 (c), and 10 mg/mL (d) of PVA₁₀₀₀ concentrations. Average particle size (at 30 °C) (e) and size ratio (at 60 °C vs. at 30 °C) (f) of PG₁₀₀₀ at various PVA concentrations.



Scheme 3. Schematic of the effect of the PVA₁₀₀₀ concentration on nanogel formation.

2.3. Effect of PVA Chain Length

To obtain stable polymer nanogels, we regulated the bridging and stabilization effects of PVA on the obtained polymer nanogels by changing the PVA chain length. We investigated the effect of the PVA chain length on the particle size and colloidal stability using

three different PVAs with varying degrees of polymerization (500: PVA₅₀₀, 1000: PVA₁₀₀₀, and 3500: PVA₃₅₀₀). When PVA with a longer chain length was used, the PVA-induced bridging effect of different polymer chains/nanogels was increased, and the large gel particles with high colloidal stability were obtained. However, the bridging effect decreased when PVA with a shorter chain length was used, and small gel particles were obtained owing to the suppression of the bridging effect of PVA.

Figure 4 shows the transmittance of the obtained polymer gel particle dispersions prepared using three different types of PVA. When the polymerization degree of PVA was increased to 3500 (PVA₃₅₀₀), the clouding-point temperature of the obtained polymer gel particles (PG₃₅₀₀) was not significantly shifted to a lower temperature compared to that of PG₁₀₀₀. Furthermore, the transmittance below the clouding-point temperature was slightly low (~75%), implying the formation of larger polymer gel particles. In fact, submicrometer-sized gel particles were obtained using PVA₃₅₀₀ (PG₃₅₀₀) below the clouding-point temperature. These results support our hypothesis that PVA assists the bridging of different polymer chains/nanogels during dispersion polymerization. Importantly, the thermoresponsiveness of PG₃₅₀₀ was different from that of PG₁₀₀₀. The particle size of PG₁₀₀₀ significantly increased above the LCST, whereas that of PG₃₅₀₀ decreased (Figure 4). This phenomenon exhibited by PG₃₅₀₀ is observed for submicrometer-sized gel particles with LCST-type thermoresponsive properties [43]. Furthermore, PG₃₅₀₀ particles showed a similar decreasing trend even in the presence of CTAB. This implies that PG₃₅₀₀ did not coagulate, but rather shrank because of dehydration above the clouding-point temperatures.

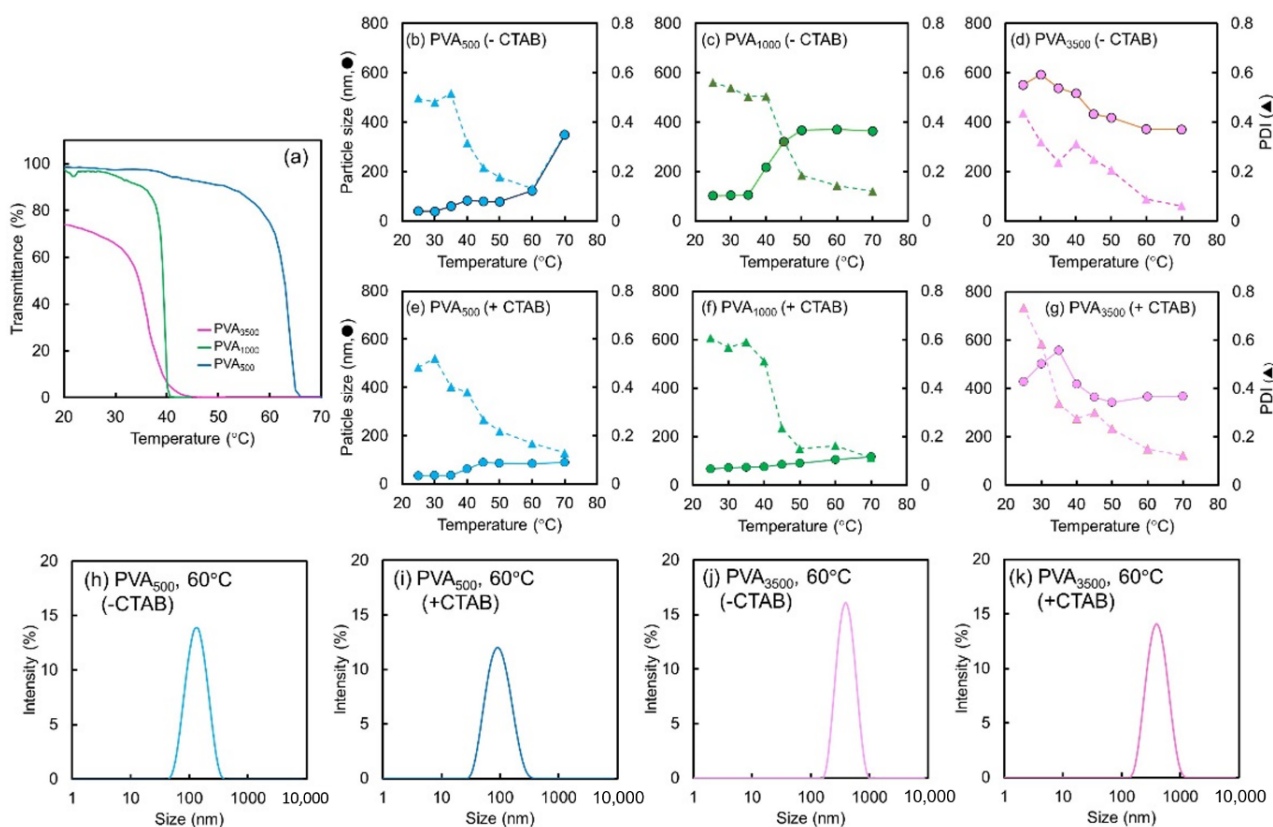


Figure 4. Transmittance of PG₅₀₀, PG₁₀₀₀, and PG₃₅₀₀ particle dispersions prepared via dispersion polymerization (a). Average particle sizes (circles) and PDI (triangles) of PG₅₀₀ (b,e), PG₁₀₀₀ (c,f), and PG₃₅₀₀ (d,g) particles at various temperatures without (b–d) or with (e–g) CTAB. Particle size distributions of PG₅₀₀ (h,i) and PG₃₅₀₀ (j,k) particles at 60 °C without (h,j) and with (i,k) CTAB. Polymer gel particles were prepared via dispersion polymerization with PVA polymer chains of different lengths (polymerization degrees: 500, 1000, and 3500) at 70 °C for 3 h.

The thermoresponsive properties and colloidal stability of the polymer gel particles prepared using PVA₅₀₀ (PG₅₀₀) were different from those of PG₁₀₀₀ and PG₃₅₀₀. The particle size of PG₅₀₀ was less than 100 nm at temperatures lower than the clouding-point temperature (Figure 4). Furthermore, the nanometer-sized polymer nanogels were clearly visible in transmittance electron microscopy images when the PNIPAm-based nanogels were prepared with PVA₅₀₀ (Figure 5). The nanometer size of PG₅₀₀ particles was maintained up to 60 °C, while the particles coagulated above 65 °C (Figure 4). The clouding-point temperature estimated from the transmittance measurements of PG₅₀₀ was approximately 63 °C, which was higher than those of PG₁₀₀₀ and PG₃₅₀₀. This may be attributed to the insertion of PVA₅₀₀ into the polymer main chains. Previous studies have revealed that the copolymerization of a hydrophilic monomer with PNIPAm shifts the LCST to a higher temperature [44]. Furthermore, a negligible increase in the particle size of PG₅₀₀ was observed above 60 °C when CTAB was added during DLS measurements. These results indicate that the increase in particle size of PG₅₀₀ (without CTAB) above 60 °C was caused by coagulation. The colloidal stability of PG₅₀₀ at high temperatures (up to 60 °C) was induced by the steric repulsion of grafted PVA₅₀₀. These results suggest that the bridging effect between the different polymer nanogels weakened with decreasing polymerization degree of PVA, whereas PVA-induced colloidal stability was afforded to the polymer nanogels. Therefore, we can conclude that the different degrees of polymerization of PVA affected the formation of polymer gel particles during dispersion polymerization by controlling the bridging effect between different polymer chains/nanogels. Furthermore, to investigate whether PVA was covalently bonded in PNIPAm nanogels, we prepared the PNIPAm nanogels with fluorescein-labeled PVA. The fluorescence spectrum of the fluorescein-labeled PVA-containing polymer gels as a dispersed state was obtained (Figure S6). The spectra clearly indicate that the PVA was covalently bonded in PNIPAm nanogels.

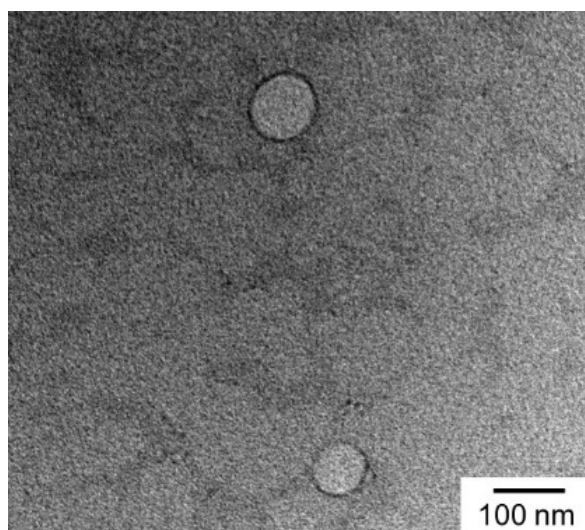


Figure 5. Transmission electron microscopy image of PG₅₀₀ prepared via dispersion polymerization with PVA₅₀₀.

3. Conclusions

In this study, we investigated the effect of PVA addition on the polymer nanogel formation during dispersion polymerization. Our results indicate that PVA induces three effects on the polymer nanogels: (i) bridging between different polymer chains formed during polymerization, (ii) stabilization of the polymer nanogels, and (iii) regulation of thermoresponsiveness. In the presence of PVA with a higher degree of polymerization (PVA₃₅₀₀), microgel particles were formed during dispersion polymerizations, owing to the enhanced bridging effect. On the contrary, the nanogels that are stable over a wide temperature range (under 60 °C) were obtained using PVA₅₀₀. The nanotechnology devel-

oped herein may help in further advancing research on polymer nanogels in fields such as biomedicine, wherein the fabrication of nanocarriers for targeted drug delivery and other similar functions may be possible.

4. Materials and Methods

4.1. Materials

NIPAm, MBAA, and potassium dihydrogen phosphate were purchased from Nacalai Tesque (Kyoto, Japan). TBAM, PVA with different degrees of polymerization and saponification, disodium hydrogenphosphate, V-50, and VA-044 were purchased from Wako Pure Chemical Co., Ltd. (Osaka, Japan). MPC, acryloxyethyl thiocarbamoyl rhodamine B, and CTAB were purchased from Sigma–Aldrich (St. Louis, MO, USA). Deionized (DI) water was obtained using a Millipore Milli-Q purification system. FAM was prepared using a previously reported procedure [9].

4.2. Apparatus

UV-visible (UV-Vis) spectral measurements were conducted using a V-560 spectrophotometer (Jasco Ltd., Tokyo, Japan). ^1H NMR spectra were measured using a 400-MHz Fourier transform (FT)-NMR apparatus (JNM-ECX400 FT-NMR system, JEOL Ltd., Tokyo, Japan). The particle size distribution and the zeta potential of the obtained particles were measured using ZETASIZER NANO-ZS (Malvern, UK).

4.3. Precipitation/Dispersion Polymerizations

NIPAm (407 mg, 3.6 mmol), TBAm (7.6 mg, 60 μmol), MPC (30 mg, 0.1 mmol), FAM (4 mg, 11 μmol), MBAA (30.8 mg, 0.2 mmol), and V-50 (217 mg, 0.8 mmol) were mixed with 10 mM phosphate buffer (pH 7.4, 100 mL) in a Schlenk flask. After N_2 /vacuum cycles, polymerization was performed at 70 $^\circ\text{C}$ for 3 h. To investigate the effect of the PVA concentration, various amounts (final concentration: 0–10 mg/mL) of PVA (polymerization degree: 1000, saponification degree: 88%) were added to the solution. To investigate the effect of the polymerization degree of PVA, the same concentrations (final concentration: 3 mg/mL) of PVA with different polymerization degrees (500, 1000, and 3500) and 88% saponification were added to the polymerization system.

4.4. Transmittance Measurements

As-prepared particle dispersions (3 mL) were poured into the UV-Vis cell, and the transmittance measurement ($\lambda = 600 \text{ nm}$) was conducted. The temperature was increased at a constant rate (0.5 $^\circ\text{C}/\text{min}$). The reversibility of the thermoresponsiveness of the obtained particles was evaluated by alternately increasing and decreasing the temperature at a constant rate (0.5 $^\circ\text{C}/\text{min}$).

4.5. Particle Size Distributions

The particle size distributions of the as-prepared particle dispersions (3 mL) were measured using DLS at different temperatures (25, 30, 35, 40, 45, 50, 60, and 70 $^\circ\text{C}$). The measurements were performed sequentially at 600 s intervals. To investigate the effect of surfactants on particle aggregation, CTAB (~1 mg/mL) was added to the particle dispersion.

Supplementary Materials: The following supporting information can be downloaded at: <https://www.mdpi.com/article/10.3390/molecules28083493/s1>. Figure S1: The ^1H -NMR spectra of precipitation polymerization, Figure S2: The ^1H -NMR spectra of dispersion polymerization with PVA, Figure S3: reversibility of the transmittance changes of polymer nanogel dispersion, Figure S4: particle size change of nanogels in the presence of cationic surfactants, Figure S5: and clouding-point temperatures of PG_{1000} prepared with different PVA_{1000} concentrations, Figure S6: Dispersion polymerization with fluorescein-labeled PVA_{500} .

Author Contributions: Conceptualization, Y.K.; Methodology, Y.K. and A.H.; Investigation, Y.K. and S.T.; Writing – original draft, Y.K.; Writing – review & editing, Y.K., S.T. and A.H.; Supervision, Y.K. All authors have read and agreed to the published version of the manuscript.

Funding: This work was partially supported by JSPS KAKENHI (Grant number 21H02004 and 22K19922), Asahi Glass Foundation, and the Leading Initiative for Excellent Young Researchers, MEXT, Japan (for Y.K.).

Institutional Review Board Statement: Not applicable.

Informed Consent Statement: Not applicable.

Data Availability Statement: The data presented in this study are available in the article.

Conflicts of Interest: The authors declare no conflict of interest.

Sample Availability: Samples of the compounds are not available from the authors.

Abbreviations

CTAB: cetyltrimethylammonium bromide; DLS, dynamic light scattering; FAM, fluorescein acrylamide; LCST, lower critical solution temperature; MBAA, *N,N'*-methylenebisacrylamide; MPC, 2-methacryloyloxyethyl phosphorylcholine; NIPAm, *N*-isopropyl acrylamide; PVA, poly(vinyl alcohol); TBAm, *t*-butyl acrylamide; V-50, 2,2'-azobis(2-methylpropionamide) dihydrochloride; NMR, nuclear magnetic resonance.

References

1. Agnihotri, S.A.; Mallikarjuna, N.N.; Aminabhavi, T.M. Recent Advances on Chitosan-Based Micro- and Nanoparticles in Drug Delivery. *J. Control. Release* **2004**, *100*, 5–28. [[CrossRef](#)] [[PubMed](#)]
2. Kono, K. Thermosensitive Polymer-Modified Liposomes. *Adv. Drug. Deliver. Rev.* **2001**, *53*, 307–319. [[CrossRef](#)] [[PubMed](#)]
3. Delcea, M.; Möhwald, H.; Skirtach, A.G. Stimuli-Responsive LbL Capsules and Nanoshells for Drug Delivery. *Adv. Drug. Deliver. Rev.* **2011**, *63*, 730–747. [[CrossRef](#)]
4. Uskokovic, V.; Lee, K.; Lee, P.P.; Fischer, K.E.; Desai, T.A. Shape Effect in the Design of Nanowire-Coated Microparticles as Transepithelial Drug Delivery Devices. *ACS Nano* **2012**, *6*, 7832–7841. [[CrossRef](#)]
5. Farokhzad, O.C.; Langer, R. Impact of Nanotechnology on Drug Delivery. *ACS Nano* **2009**, *3*, 16–20. [[CrossRef](#)]
6. Veisoh, O.; Gunn, J.W.; Zhang, M.Q. Design and Fabrication of Magnetic Nanoparticles for Targeted Drug Delivery and Imaging. *Adv. Drug. Deliver. Rev.* **2010**, *62*, 284–304. [[CrossRef](#)]
7. Kataoka, K.; Harada, A.; Nagasaki, Y. Block Copolymer Micelles for Drug Delivery: Design, Characterization and Biological Significance. *Adv. Drug. Deliver. Rev.* **2012**, *64*, 37–48. [[CrossRef](#)]
8. Sharma, B.; Striegler, S. Nanogel Catalysts for the Hydrolysis of Underivatized Disaccharides Identified by a Fast Screening Assay. *ACS Catalysis* **2023**, *13*, 1614–1620. [[CrossRef](#)]
9. Akl, M.A.; Sarhan, A.A.; Shoueir, K.R.; Atta, A.M. Application of Crosslinked Ionic Poly(Vinyl Alcohol) Nanogel as Adsorbents for Water Treatment. *J. Dispers. Sci. Technol.* **2013**, *34*, 1399–1408. [[CrossRef](#)]
10. Richa; Roy Choudhury, A. Synthesis of a Novel Gellan-Pullulan Nanogel and Its Application in Adsorption of Cationic Dye from Aqueous Medium. *Carbohydr. Polym.* **2020**, *227*, 115291. [[CrossRef](#)] [[PubMed](#)]
11. Asua, J.M. Miniemulsion Polymerization. *Prog. Polym. Sci.* **2002**, *27*, 1283–1346. [[CrossRef](#)]
12. Landfester, K. Miniemulsion Polymerization and the Structure of Polymer and Hybrid Nanoparticles. *Angew. Chem. Int. Ed.* **2009**, *48*, 4488–4507. [[CrossRef](#)] [[PubMed](#)]
13. Pan, G.; Sudol, E.D.; Dimonie, V.L.; El-Aasser, M.S. Nitroxide-Mediated Living Free Radical Miniemulsion Polymerization of Styrene. *Macromolecules* **2001**, *34*, 481–488. [[CrossRef](#)]
14. Kitayama, Y.; Yorizane, M.; Minami, H.; Okubo, M. Preparation of Block Copolymer Particles by Two-Step, Reversible Chain Transfer Catalyzed Polymerization (RTCP) with Nitrogen Catalyst in Miniemulsion Systems. *Polym. Chem.* **2012**, *3*, 1394–1398. [[CrossRef](#)]
15. Sudol, E.D.; Daniels, E.S.; El-Aasser, M.S. Overview of Emulsion Polymerization—Stepping toward Prediction. *ACS Symp. Ser.* **1992**, *492*, 1–11.
16. Ferguson, C.J.; Hughes, R.J.; Nguyen, D.; Pham, B.T.T.; Gilbert, R.G.; Serelis, A.K.; Such, C.H.; Hawket, B.S. Ab Initio Emulsion Polymerization by RAFT-Controlled Self-Assembly. *Macromolecules* **2005**, *38*, 2191–2204. [[CrossRef](#)]
17. Thickett, S.C.; Gilbert, R.G. Emulsion Polymerization: State of the Art in Kinetics and Mechanisms. *Polymer* **2007**, *48*, 6965–6991. [[CrossRef](#)]
18. Smith, W.V.; Ewart, R.H. Kinetics of Emulsion Polymerization. *J. Chem. Phys.* **1948**, *16*, 592–599. [[CrossRef](#)]

19. Kitayama, Y.; Okubo, M. A synthetic Route to Ultra-High Molecular Weight Polystyrene (>10⁶) with Narrow Molecular Weight Distribution by Emulsifier-Free, Emulsion Organotellurium-Mediated Living Radical Polymerization (emulsion TERP). *Polym. Chem.* **2016**, *7*, 2573–2580. [[CrossRef](#)]
20. Khan, M.; Guimarães, T.R.; Kuchel, R.P.; Moad, G.; Perrier, S.; Zetterlund, P.B. Synthesis of Multicompositional Onion-like Nanoparticles via RAFT Emulsion Polymerization. *Angew. Chem. Int. Ed.* **2021**, *60*, 23281–23288. [[CrossRef](#)]
21. Schmid, A.; Fujii, S.; Armes, S.P.; Leite, C.A.P.; Galembeck, F.; Minami, H.; Saito, N.; Okubo, M. Polystyrene—Silica Colloidal Nanocomposite Particles Prepared by Alcoholic Dispersion Polymerization. *Chem. Mater.* **2007**, *19*, 2435–2445. [[CrossRef](#)]
22. Kawaguchi, S.; Ito, K. Dispersion Polymerization. In *Polymer Particles*; Okubo, M., Ed.; Springer: Berlin/Heidelberg, Germany, 2005; Volume 175, pp. 299–328.
23. Paine, A.J.; Luymes, W.; McNulty, J. Dispersion Polymerization of Styrene in Polar Solvents. 6. Influence of Reaction Parameters on Particle Size and Molecular Weight in Poly(N-vinylpyrrolidone)-Stabilized Reactions. *Macromolecules* **1990**, *23*, 3104–3109. [[CrossRef](#)]
24. Tseng, C.M.; Lu, Y.Y.; El-Aasser, M.S.; Vanderhoff, J.W. Uniform Polymer Particles by Dispersion Polymerization in Alcohol. *J. Polym. Sci. Part A Polym. Chem.* **1986**, *24*, 2995–3007. [[CrossRef](#)]
25. Wang, J.; Cormack, P.A.G.; Sherrington, D.C.; Khoshdel, E. Monodisperse, Molecularly Imprinted Polymer Microspheres Prepared by Precipitation Polymerization for Affinity Separation Applications. *Angew. Chem. Int. Ed.* **2003**, *42*, 5336–5338. [[CrossRef](#)]
26. Li, W.H.; Stöver, H.D.H. Porous Monodisperse Poly(divinylbenzene) Microspheres by Precipitation Polymerization. *J. Polym. Sci. A Polym. Chem.* **1998**, *36*, 1543–1551. [[CrossRef](#)]
27. Bai, F.; Yang, X.; Huang, W. Synthesis of Narrow or Monodisperse Poly(divinylbenzene) Microspheres by Distillation-Precipitation Polymerization. *Macromolecules* **2004**, *37*, 9746–9752. [[CrossRef](#)]
28. Yoshimatsu, K.; Reimhult, K.; Krozer, A.; Mosbach, K.; Sode, K.; Ye, L. Uniform Molecularly Imprinted Microspheres and Nanoparticles Prepared by Precipitation Polymerization: The Control of Particle Size Suitable for Different Analytical Applications. *Anal. Chim. Acta* **2007**, *584*, 112–121. [[CrossRef](#)]
29. Okaya, T.; Fujita, H.; Suzuki, A.; Kikuchi, K. Study on Chain Transfer Reaction of Poly(vinyl acetate) Radical with Poly(vinyl alcohol) in a Homogeneous System. *Des. Monomers Polym.* **2004**, *7*, 269–276. [[CrossRef](#)]
30. Lee, A.; Tsai, H.Y.; Yates, M.Z. Steric Stabilization of Thermally Responsive N-Isopropylacrylamide Particles by Poly(vinyl alcohol). *Langmuir* **2010**, *26*, 18055–18060. [[CrossRef](#)]
31. Tang, Z.; Weng, J.; Guan, Y.; Zhang, Y. Unexpected Large Depression of VPTT of a PNIPAM Microgel by Low Concentration of PVA. *Macromol. Chem. Phys.* **2017**, *218*, 1700364. [[CrossRef](#)]
32. Matsumura, Y.; Maeda, H. A New Concept for Macromolecular Therapeutics in Cancer-Chemotherapy—Mechanism of Tumor-tropic Accumulation of Proteins and the Antitumor Agent Smancs. *Cancer Res.* **1986**, *46*, 6387–6392. [[PubMed](#)]
33. Blackburn, W.H.; Lyon, L.A. Size-Controlled Synthesis of Monodisperse Core/Shell Nanogels. *Colloid Polym. Sci.* **2008**, *286*, 563–569. [[CrossRef](#)]
34. Takeuchi, T.; Kitayama, Y.; Sasao, R.; Yamada, T.; Toh, K.; Matsumoto, Y.; Kataoka, K. Molecularly Imprinted Nanogels Acquire Stealth in situ by Cloaking Themselves with Native Dysopsonic Proteins. *Angew. Chem. Int. Ed.* **2017**, *56*, 7088–7092. [[CrossRef](#)]
35. Ichikawa, S.; Shimokawa, N.; Takagi, M.; Kitayama, Y.; Takeuchi, T. Size-Dependent Uptake of Electrically Neutral Amphipathic Polymeric Nanoparticles by Cell-Sized Liposomes and an Insight into Their Internalization Mechanism in Living Cells. *Chem. Commun.* **2018**, *54*, 4557–4560. [[CrossRef](#)]
36. Morishita, T.; Yoshida, A.; Hayakawa, N.; Kiguchi, K.; Cheubong, C.; Sunayama, H.; Kitayama, Y.; Takeuchi, T. Molecularly Imprinted Nanogels Possessing Dansylamide Interaction Sites for Controlling Protein Corona in Situ by Cloaking Intrinsic Human Serum Albumin. *Langmuir* **2020**, *36*, 10674–10682. [[CrossRef](#)]
37. Cheubong, C.; Yoshida, A.; Mizukawa, Y.; Hayakawa, N.; Takai, M.; Morishita, T.; Kitayama, Y.; Sunayama, H.; Takeuchi, T. Molecularly Imprinted Nanogels Capable of Porcine Serum Albumin Detection in Raw Meat Extract for Halal Food Control. *Anal. Chem.* **2020**, *92*, 6401–6407. [[CrossRef](#)]
38. Hayakawa, N.; Yamada, T.; Kitayama, Y.; Takeuchi, T. Cellular Interaction Regulation by Protein Corona Control of Molecularly Imprinted Polymer Nanogels Using Intrinsic Proteins. *ACS Appl. Polym. Mater.* **2020**, *2*, 1465–1473. [[CrossRef](#)]
39. Hayakawa, N.; Kitayama, Y.; Igarashi, K.; Matsumoto, Y.; Takano, E.; Sunayama, H.; Takeuchi, T. Fc Domain-Imprinted Stealth Nanogels Capable of Orientational Control of Immunoglobulin G Adsorbed in Vivo. *ACS Appl. Mater. Interfaces* **2022**, *14*, 16074–16081. [[CrossRef](#)] [[PubMed](#)]
40. Kitayama, Y.; Yamada, T.; Kiguchi, K.; Yoshida, A.; Hayashi, S.; Akasaka, H.; Igarashi, K.; Nishimura, Y.; Matsumoto, Y.; Sasaki, R.; et al. In vivo Stealthified Molecularly Imprinted Polymer Nanogels Incorporated with Gold Nanoparticles for Radiation Therapy. *J. Mater. Chem. B* **2022**, *10*, 6784–6791. [[CrossRef](#)]
41. Kayal, S.; Ramanujan, R.V. Doxorubicin Loaded PVA Coated Iron Oxide Nanoparticles for Targeted Drug Delivery. *Mater. Sci. Eng. C* **2010**, *30*, 484–490. [[CrossRef](#)]
42. Deng, J.; Yuk, H.; Wu, J.; Varela, C.E.; Chen, X.; Roche, E.T.; Guo, C.F.; Zhao, X. Electrical Bioadhesive Interface for Bioelectronics. *Nat. Mater.* **2021**, *20*, 229–236. [[CrossRef](#)] [[PubMed](#)]

43. Yin, J.; Hu, H.; Wu, Y.; Liu, S. Thermo- and Light-Regulated Fluorescence Resonance Energy Transfer Processes within Dually Responsive Microgels. *Polym. Chem.* **2011**, *2*, 363–371. [[CrossRef](#)]
44. Perelman, L.A.; Moore, T.; Singelyn, J.; Sailor, M.J.; Segal, E. Preparation and Characterization of a pH- and Thermally Responsive Poly(N-isopropylacrylamide-coacrylic acid)/Porous SiO₂ Hybrid. *Adv. Funct. Mater.* **2010**, *20*, 826–833. [[CrossRef](#)] [[PubMed](#)]

Disclaimer/Publisher’s Note: The statements, opinions and data contained in all publications are solely those of the individual author(s) and contributor(s) and not of MDPI and/or the editor(s). MDPI and/or the editor(s) disclaim responsibility for any injury to people or property resulting from any ideas, methods, instructions or products referred to in the content.